Improving Thermal Estimates for Student-Built CubeSats

Dhrumil Patadia[1], *Ines Uriol Balbin*[2], *Sevket Uludag*[3], *Stefano Speretta*[3]

Abstract

CubeSats, particularly those developed by student teams, often face extremely short development cycles, leading to limited attention to detailed thermal analysis. Accurate thermal modelling is important to ensure the reliable operation of on-board systems. However, professional thermal modelling tools such as ESATAN are complex, and correlation-based validation methods are time-consuming and resource-intensive. Consequently, small satellite teams frequently rely on simplified models with large error margins in temperature predictions.

This paper presents the design of experiments to determine thermo-optical properties for materials commonly used in student CubeSat construction. Additionally, a database is presented that highlights the thermal conductivity, solar absorptivity, heat capacity and infra-red emissivity, obtained from the experiments, for printed circuit boards (PCBs), solar cells and solar panels. Finally, a sensitivity analysis is performed to indicate the effect of the uncertainties in property values on the average battery temperature as it is a thermally critical component.

The design of experiments can be used by student teams to perform their own experiments and the properties obtained in this work can be used for their initial thermal design. This will allow student teams to make better estimates for the thermal budget of their CubeSat missions.

Keywords
Thermal Testing, ESATAN-TMS, CubeSats, Student Teams

[1] Corresponding author: Delft University of Technology, Netherlands, d.patadia@student.tudelft.nl
[2] Aerospace Structures & Materials, Aerospace Engineering, Delft University of Technology, Netherlands
[3] Space Engineering, Aerospace Engineering, Delft University of Technology, Netherlands

DOI: 10.14459/2026md1857518

Nomenclature

$A(\lambda)$: absorbance (raw data)

C_P: heat capacity

I: intensity measured by sensor

I_o: incident intensity

k: thermal conductivity

$\alpha(\lambda)$: fraction of light absorbed

α_S: effective solar absorptivity

ε_{IR}: infrared emissivity

E_λ: solar spectral irradiance

$r(\lambda)$: fraction of light reflected

Q_{rad}: Radiation heat flow

Abbreviations

PCB: Printed circuit board

IR: Infrared

TC: Thermocouples

TU: Technical University

PQ: pocketcube

1. Introduction

For CubeSats, thermal control is more difficult because they are small, have limited surface area to reject heat, and have low available power for active systems [1][2]. Therefore, their thermal performance depends mainly on good design choices and proper material selection from the beginning. Although advanced software tools such as ESATAN-TMS and Thermal Desktop can perform detailed thermal analysis, they require significant time and experience to use.

SmallSats developed by student teams often give low priority to thermal analysis and design due to lack of funds, development time and experience with thermal analysis software [3].

Guerra et al. [6] also highlight how CubeSats are built using components off the shelf and that thermal control engineering in these projects is overlooked due to the time required and its complexity. Other examples that highlight these issues are student CubeSats such as the ones from Technical University (TU) Delft [4] and TU Darmstadt [5].

The student team at TU Darmstadt could not perform a proper thermal analysis due to software licensing issues and had to rely on a MATLAB code available which imposed certain limitations on the way the configuration can be defined and the lack of attitude modification of the satellite [5].

TU Delft pocketcube (PQ), Delfi-PQ, experienced “unforeseen problems” [4] which led the electrical power sub system to operate from -10°C to 25°C, instead of the planned range of 5°C to 40°C.

While literature provides a reference for thermo-optical values, the sensitivity of CubeSat temperatures to external surface properties, combined with the high variability of thermal properties, results in large observed discrepancies in flight missions such as Delfi-PQ [7].

Therefore, an experimentally validated database of thermo-optical properties for commonly used CubeSat components is necessary. To address these issues, this work aims to determine thermal (k & C_P) and optical (α_S & ε_{IR}) properties for commonly used components like PCBs, solar panels and solar cells used by the student teams at TU Delft. This paper is a part of the ongoing thesis work at TU Delft. The progress made so far has been shared in this paper.

2. Design of Experiments

To measure the thermal and optical properties of the selected components different tests were designed and executed. First, solar absorptivity was measured using a spectrometer (2.1). Secondly, k, ε_{IR} and C_P were measured using thermal balance tests (2.2). Finally, an infrared camera was used to measure the emissivity of the solar cells.

2.1. Solar absorptivity test

Solar absorptivity has been measured using the Lambda 1050 S spectrometer with an integrating sphere. The machine gives raw data of absorbance for each wavelength which must be converted into the effective solar absorptance of the sample. The procedure is shown below.

$$A(\lambda) = -log_{10}(\frac{I}{I_o}) \qquad (1)$$

The ratio $\frac{I}{I_o}$ represents the reflection ratio, r

$$A(\lambda) = -log_{10}(r(\lambda)) \qquad (2)$$

$$r(\lambda) = 10^{-A(\lambda)} \qquad (3)$$

$$\alpha(\lambda) = 1 - r(\lambda) = 1 - 10^{-A(\lambda)} \quad (4)$$

The effective solar absorptivity is then calculated as

$$\alpha_S = \frac{\Sigma\, \alpha(\lambda) * E_\lambda}{\Sigma E_\lambda} \quad (5)$$

E_λ can be obtained from the work done by Gueymard [8].

This test was done for solar cells, green, white and black solar panels having dimensions of approximately 30mm × 30mm.

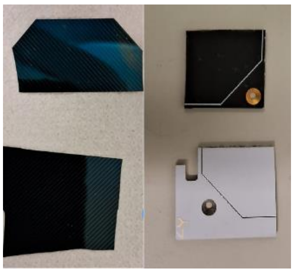

Figure 1. Solar Cell and Solar Panel

2.2. *Thermal Balance tests*

Thermal balance tests, inside the vacuum chamber, have been performed for the determination of thermal conductivity, heat capacity and infrared emissivity. For these tests, heat is provided using a tape heater and temperatures along the surface of the sample are measured using thermocouples. It is important to account for heat loss from heater. The heat loss calculations have been shown in the Appendix.

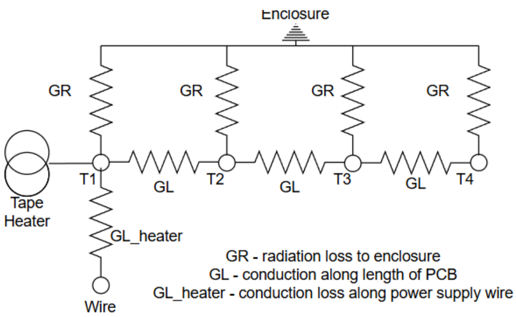

Figure 2. Thermal network – PCB

This thermal network represents the thermal balance test set-up as shown in Figure *3*.

The test was carried out inside a vacuum chamber, and the setup was enclosed by a box (shown in *Figure 3*) whose surface had a known emissivity ($\varepsilon_{IR} = 0.8$) to account for the radiative exchange factor. During this test, 0.5W of power was supplied to the heater and the steady state temperatures of the samples were recorded.

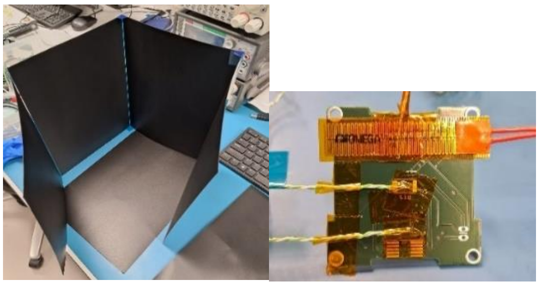

Figure 3. Enclosure ($\varepsilon_{IR} = 0.8$) and PCB Test 1 setup

For representation purposes, the thermal network (*Figure 2*) considers the PCB to be divided into 4 elements. For this thermal balance test, referred to as **Test 1**, during the steady state heat flows through three paths: Heat loss from heater, Conduction along the length of PCB, and Radiation from the surface of the PCB

Of these three paths for the heat flow, two of them: the radiation and conduction of the sample are unknown. This makes the steady state heat balance equation unsolvable as there are two unknowns.

To solve this problem, another thermal balance test was conducted for the same setup, say, **Test 2**. The only difference between both tests was that test **1** was with a bare PCB, while test **2** was with the paint ($\varepsilon_{IR} = 0.8$) coated PCB. This meant that the only unknown in test 2 was the thermal conductivity.

Now, the steady state thermal balance equation for this can be used to determine this thermal conductivity. Further, this value from **Test 2** can be fed to the data obtained from **Test 1** to determine the infrared emissivity of the PCB.

Figure 4. PCB with LabIR paint of known emissivity (ε_{IR} = 0.8) for Test 2

Finally, for determination of the heat capacity (C_P), the heater was turned off at the end of steady state and the time taken for the PCB to

DOI: 10.14459/2026md1857518

reach back to room temperature was recorded. A code was written to model this transient phase which gave the heat capacity of the sample.

The exact same procedure has been followed to determine properties of the black solar panel. The green and the white solar panel are considered to have the same thermal properties as only the surface paint varies amongst them.

For all these tests, the error sources have been identified and uncertainties in measurements have been propagated from TC accuracy (±2.2K), paint emissivity (±0.013), length and power supply measurements

2.3. Test with Infrared camera

This test includes a solar cell sample attached to a tape heater whose temperature was measured using a thermocouple (*Figure 5*).

Figure 5. Solar cell test setup for IR camera measurement

By changing the power given to the sample via the heater two different temperature states were considered. At both power levels, the temperature is measured both via the infrared camera as well as the thermocouple. The only constant is the surrounding radiation reflected by the solar cell. With these data the infrared emissivity of the sample can be calculated assuming it is constant at both temperatures.

3. Results and Discussion

Table 1. Database of properties

Sample	α_S	ε_{IR}	k	C_P
Solar cell (A)	0.90	0.93	-	-
Solar cell (B)	0.834	0.93	-	-
PCB	-	0.84	10	550
Black solar panel	0.77	0.92	25	660
White solar panel	0.33	-	25	660
Green solar panel	0.32	-	25	660

In the above table, the unit of k is $Wm^{-1}K^{-1}$ and Cp is J$kg^{-1}K^{-1}$

The table above gives the nominal values of properties. The further discussion will highlight the uncertainty in the values obtained.

3.1. Solar absorptivity

The measured values of solar absorptivity and the reference values that were used in previous CubeSats developed by TU Delft are shown in *Table 2*. Looking at the values obtained for the solar cells and the black solar panel (used in Delfi-PQ), they are lower than the reference value. This is one of the factors that could have contributed to Delfi-PQ experiencing a lower temperature than expected as discussed in the introduction.

Another important aspect to note is the variation in the solar absorptivity of the white solar panel. Nasa [15] highlights that white coatings can have a wide range of values for solar absorptivity from 0.17 to 0.39. Thus, it is important to measure the value, if white solar panels are being used, as manufacturers would usually not provide this value.

Table 2. Solar absorptivity values

Component	Measured α_S	Reference	Variation
Solar cell	0.902 (Sample A)	<0.91 [9]	0.8%
	0.834 (Sample B)		8.4%
Black Solar Panel	0.867	0.94 [10]	7.8%
White Solar panel	0.331	0.21 [10]	57%
Green Solar Panel	0.324	-	

3.2. PCB properties

The measurements made for the PCB and the reference values found in literature are shown in Table 3.

Table 3. PCB measured properties

Property	Measured Value	Reference Value
k ($Wm^{-1}K^{-1}$)	10 ± 5	17.7 [12]
C_P ($Jkg^{-1}K^{-1}$)	550 ± 40	589 [7]
ε_{IR} (-)	0.86 ± 0.06	0.8 to 0.91 [13]

The measured thermal conductivity is approximately 40% lower than the value commonly reported in the literature. A comparison with additional literature sources [14] also indicates that the obtained value is lower than expected. The error could be due to multiple reasons: error in heat loss estimation or heat leak through thermocouple cables. The

DOI: 10.14459/2026md1857518

experiment was repeated, and similar temperature distributions were observed, suggesting that the deviation is likely not due to random measurement error. Instead, it may indicate a lower copper content in the tested PCB than assumed which can differ between suppliers and even between production batches from the same supplier.

The source of uncertainty stems from the variability of heat loss and thermocouple accuracy of ±2.2K.

3.3. Solar panel properties

The measurements made for the solar panel are shown in *Table 4*.

Table 4. Solar Panel measured properties

Property	Measured Value	Reference Value
k $(Wm^{-1}K^{-1})$	25 ± 15	34 [12]
C_P $(Jkg^{-1}K^{-1})$	660 ± 130	575 [7]
ε_{IR} (-)	0.92 ± 0.03	Close to unity [10]

The solar panel used has a copper content around 2 times that of the PCB, thus a value of thermal conductivity close to 25 W/mK is justifiable.

3.4. Solar cell properties

The solar cell is adhesively attached to the solar panel, and it is very thin and light compared to the panel, thus its thermal conductivity and heat capacity will not be considered. But it covers a major portion in terms of area of the solar panel, thus its solar absorptivity and infrared emissivity are of utmost importance.

Property	Measured Value	Reference Value
ε_{IR} (-)	0.93 ± 0.07	Close to unity [10]

The measurements from the thermal camera had high uncertainty and this led to an emissivity range between 0.86 and 1 which makes the results not useful. This is because of the accuracy of TC (±2.2K) and camera(±3K).

4. Sensitivity Analysis

The experimentally obtained properties were used in the thermal model of Delfi-PQ, and their uncertainties were applied as bounds to determine temperature sensitivities.

One-at-a-time sensitivity analysis was carried with the parameters listed in *Table 5* and the average battery temperature, being a thermally critical component, was observed.

Table 5. Properties for Sensitivity Analysis

Component	Property	Value
PCB	C_P $(Jkg^{-1}K^{-1})$	550 ± 40
	ε_{IR} (-)	0.86 ± 0.06
Solar Panel	C_P $(Jkg^{-1}K^{-1})$	660 ± 130
	ε_{IR} (-)	0.9 ± 0.1
	α_S (-)	0.77 ± 0.1
Solar Cell	ε_{IR} (-)	0.93 ± 0.07
	α_S (-)	0.61* ± 0.03

* Considering 30 % solar cell efficiency

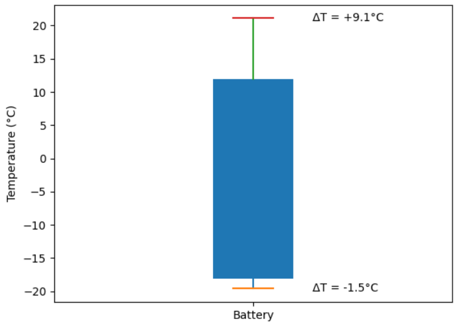

Figure 6. Battery temperature deviation due to uncertainties in properties

The blue boxplot indicates the average temperature of the battery if nominal values of properties mentioned in *Table 5* are used. The deviations on either side of +9.1°C and -1.5°C arise due to uncertainties in properties. Thus, student teams should account for these in their thermal models when considering the nominal working temperatures usually given by manufacturers.

5. Future work and conclusions

This study experimentally determined thermo-optical and thermal properties for PCB and solar panel components commonly used in student-built CubeSats. Solar absorptivity measurements showed deviations of up to 7–8% compared to reference values previously adopted in CubeSat thermal models. More significantly, the measured thermal conductivity of the PCB was approximately 40% lower than commonly cited literature values. Although measurement uncertainties exist, repeated experiments produced consistent temperature distributions, indicating that the deviation is likely linked to material composition variability, such as copper content or supplier-dependent FR4 properties.

These results highlight the risk of directly adopting literature values for preliminary thermal modelling without validation.

DOI: 10.14459/2026md1857518

The experimental approach presented here demonstrates a practical method for student teams to obtain more representative material properties using accessible laboratory equipment.

The next phase of the research will focus on development of reduced-order thermal models.

Appendix

For the determination of heat loss, the heater was attached to a piece of solar panel having the same dimensions as the heater. Both the heater and the solar panel were covered with LabIR paint [11] to ensure a known emissivity ($\varepsilon_{IR} = 0.8$). The test was conducted at a pressure of 0.12mbar (lowest achievable in the vacuum chamber available).

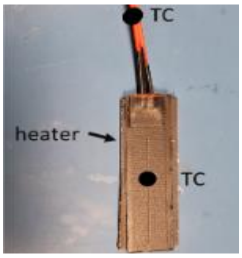

Figure 7. Heat loss estimation test setup

Table 6. Heat loss estimation

Power Input	Heater Temp.	Wire Temp.	Q_{rad}	Heat loss
0.5W	45°C	30°C	0.2W	0.3W
1.5W	92°C	40°C	0.74W	0.76W

This heat loss data gives an effective heat loss coefficient of 0.015 ± 0.006 WK^{-1}.

References

[1] European Cooperation for Space Standardization, *ECSS-E-ST-31C: Space engineering – Thermal control general requirements*, 15 Nov. 2008.

[2] National Aeronautics and Space Administration, “7.0 Thermal control,” in *State-of-the-Art Small Spacecraft Technology Report 2024 Edition*, Feb. 5, 2025.

[3] A. Alanazi and J. Straub, “Engineering methodology for student-driven CubeSats,” Aerospace, vol. 6, 5 2019.

[4] Z. Zhang and S. Speretta, “Orbital Temperature Model Construction for Delfi-PQ,” TU Delft, technical report.

[5] J. Gomez, “Thermal Analysis, Design and Verification of an Academic CubeSat Mission in a MBSE Context,”, master thesis, TU Darmstadt, 2024.

[6] A. G. C. Guerra, D. Nodar-Lopez, and R. Pardavila, “Thermal analysis of the electronics of a CubeSat mission,” arXiv, 2018.

[7] R. ´Avila De Luis, “Standardized Thermal Control Solutions for Pocketcubes,” TU Delft, 2019

[8] C. A. Gueymard, “Revised composite extraterrestrial spectrum based on recent solar irradiance observations,” Solar Energy, vol. 169, pp. 434–440, 7 2018.

[9] “Azur Space: Triple Junction GaAs Solar Cell,”,https://www.azurspace.com/media/uploads/file_links/file/bdb_00010891-01-00_tj3g30-advanced_4x8.pdf, last visited: 28-02-2026.

[10] V. N. Gorev, et al. “The effect of the PCB solder mask type of the hull outer surface of the CubeSat 3U on its thermal regime,” IOP, 2020

[11] LabIR Paints, https://paints.labir.cz/en/paints/herp-ht/, last visited: 28-02-2026.

[12] K. Azar and J. E. Graebner, “Experimental determination of thermal conductivity of printed wiring boards,” Annual IEEE Semiconductor Thermal Measurement and Management Symposium, pp. 169–182, 1996.

[13] M. M. Finckenor and R. F. Coker, “Optical Properties of Nanosatellite Hardware,” NASA NTRS, 2014.

[14] A. K. Te Nijenhuis, et al., “Thermal Analysis and Verification of CubeSat Designs with ESATAN-TMS,” in 50th ICES, vol. 104, pp. 12–15, 2021

[15] L. Kauder, “Spacecraft Thermal Control Coatings References,” Technology Report, NASA, 2005.